APPLICATION NOTE 6433

UNDERSTANDING PENETRATION DEPTH VS. WAVELENGTH FOR BIOSENSOR APPLICATIONS

Abstract: As visible and infrared waves penetrate human skin, absorption and scattering in the skin layers occurs. The penetration depth of the waves depends on the wavelength and properties of each skin layer. Formulas are presented for generating the absorption and scattering properties as a function of wavelength for each layer of the skin. These properties can then be modeled to determine penetration depth of various wavelengths into human skin. By understanding penetration depth as a function of wavelength, the optimal wavelength can be selected for specific biosensor applications.

Introduction

Knowledge of the behavior of light as it impinges upon and travels through the skin is crucial for optimizing optical biosensors because it allows for accurate simulation of penetration depth as a function of wavelength. This application note reviews the absorption and reduced scattering coefficients of human skin layers as a function of wavelength. Using these coefficients, penetration depth as a function of wavelength can be simulated and the optimal light source wavelength can be chosen for a given biosensor application.

Simulating Light Transport Through the Skin

Skin consists of three main layers from the surface: the blood-free epidermis layer (100µm thick), vascularized dermis layer (1mm to 2mm thick), and subcutaneous adipose tissue (from 1mm to 6mm thick, depending on the body site). Typically, the optical properties of these layers are characterized by absorption μ_a and scattering μ_s coefficients and the anisotropy factor *g*. The absorption coefficient characterizes the average number of absorption events per unit path length of photons travelling in the tissue. The main absorbers in the visible spectral range are the blood, hemoglobin, β-carotene, and bilirubin. In the IR spectral range, absorption properties of skin dermis are dominated by absorption of water. The scattering coefficient characterizes the average number of scattering events per unit path length of photons travelling in the tissue, and the anisotropy factor *g* represents the average cosine of the scattering angles.

In the following sections, we outline the biological characteristics of each layer and how they affect the propagation and absorption of light.

Skin Structure and Optical Model

The first and outermost section of human skin is the epidermis. The epidermis can be subdivided into two sublayers: nonliving and living epidermis. Nonliving epidermis or stratum corneum (about 20µm thick) is composed mainly of dead cells, which are highly keratinized with high lipid and protein content. It also has a relatively low water content[1]. Light absorption in this tissue is low and relatively uniform in the visible region.

The living epidermis (100µm thick) propagates and absorbs light. The absorption properties are mainly determined by a natural chromophore, melanin[2]. There are two types of melanin: a red/yellow pheomelanin and a brown/black eumelanin, which is associated with skin pigmentation. The melanin absorption level depends on how many melanosomes per unit volume are present. Typically, the volume fraction of the epidermis occupied by melanosomes varies from 1% (lightly pigmented specimens) to 40% (darkly pigmented specimens). The scattering properties of melanin particles are dependent on particle size and can be predicted by the Mie theory.

The dermis is a 0.6mm to 3mm thick structure composed of dense, irregular connective tissue containing nerves and blood vessels. The dermis can be divided into two layers based on the size of the blood vessels[3]. Smaller vessels lie closer to the skin surface in the papillary dermis while larger blood vessels populate the deeper reticular dermis. Absorption in the dermis is defined by the absorption of hemoglobin, water, and lipids. Since oxyhemoglobin and deoxyhemoglobin have different absorption profiles, the oxygen saturation must be known. For an adult, the arterial oxygen saturation is generally above 95%[4]. Typical venous oxygen saturation is 60% to 70%[5].

The scattering properties of the dermal layers are mainly defined by the fibrous structure of the tissue. Light can scatter on interlaced collagen fibrils and bundles as well as single collagen fibrils. Since the dermal layer is relatively thick compared to the epidermis, the average scattering properties of the skin are dominated by dermal scattering.

The subcutaneous adipose tissue is formed by a collection of fat cells containing stored fat (lipids). Its thickness varies considerably throughout the body: from nonexistent in the eyelids to up to 3cm thick in the abdomen. Absorption of the human adipose tissue is defined by absorption of hemoglobin, lipids and water. The main scatterers of adipose tissue are spherical droplets of lipids, which are uniformly distributed within the fat cells. The diameters of the adipocytes are in the range 15µm to 250µm[6] and their mean diameter ranges from 50µm to 120µm[7]. In the spaces between the cells there are blood capillaries, nerves, and reticular fibrils connecting each cell and providing metabolic activity to the fat tissue.

In this application note, we present a planar five-layer optical model of human skin (see **Figure 1**) based on the stratified skin layers outlined above. The layers included in the model are the stratum corneum, the living epidermis, the two layers of dermis (papillary and reticular), and the subcutaneous adipose tissue layer. Thickness of the layers as well as typical ranges of blood, water, lipids, and melanin contents, and refractive indices of the layers and mean vessel diameters are presented in **Table 1**.
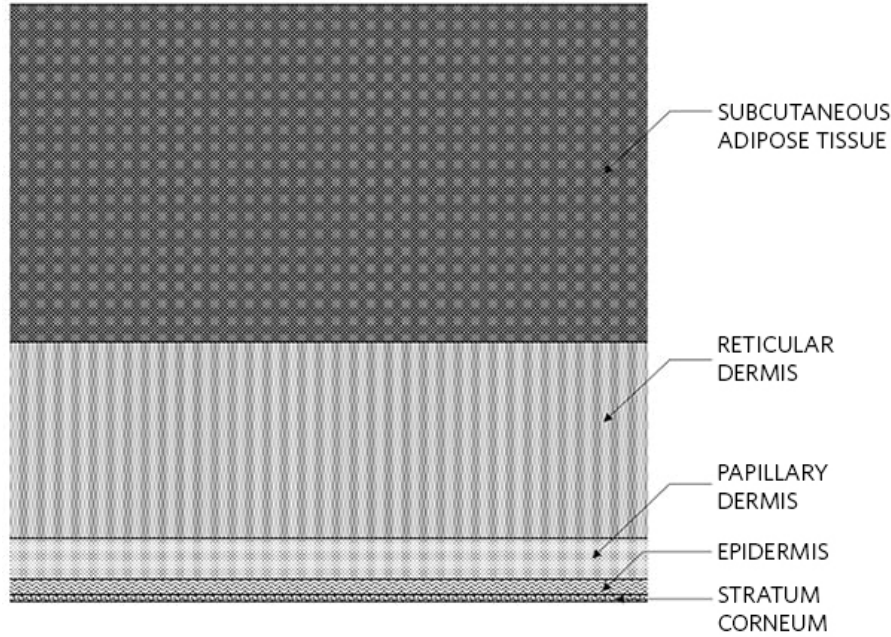

Figure 1. The five-layer optical model of the skin (not to scale).

Table 1. Parameters of Skin Layers Used in the Simulation

Skin layers	Thickness (mm)	Refractive index	Volume fraction of (%)				Scattering coefficient at 577nm (bloodless) (cm-1)	Mean vessel diameter (μm)
			Melanosomes	Blood	Water	Lipids		
Stratum Corneum	0.01	1.55	0.00	0.00	35.00	20.00	300	0
Epidermis	0.1	1.44	1-10	0.00	60.00	15.10	300	0
Papillary Dermis	0.2	1.39	0.00	0.2–4	50.00	17.33	120	6
Reticular Dermis	1.8	1.41	0.00	0.2–5	70.00	17.33	120	15
Subcutaneous Adipose Tissue	3	1.44	0.00	5.00	5.00	75–95	130	75

Absorption

In the visible and NIR spectral ranges, the absorption coefficient of each layer includes contributions from eumelanin, pheomelanin, oxyhemoglobin, deoxyhemoglobin, bilirubin, β-carotene, lipids, and water. The spectral extinction coefficients for these pigments, denoted by $\epsilon eu(\lambda), \epsilon ph(\lambda), \epsilon ohb(\lambda), \epsilon dhb(\lambda), \epsilon bil(\lambda),$ and $\epsilon \beta(\lambda)$, respectively, are given from the curves shown in **Figure 2**. The total absorption coefficient for the kth layer is given by:

$$\mu a_k(a_{k,eu}(\lambda))\vartheta_{k,mel}+(a_{k,ohb}(\lambda)+a_{k,dhb}(\lambda)+a_{k,bil}(\lambda))\vartheta_{k,blood}$$

$$+ (a_{k,eu}(\lambda))\vartheta_{k,water} + (a_{k,lip}(\lambda))\vartheta_{k,lip}$$

$$+ (a_{base}(\lambda) + a_{k,\beta}(\lambda))(1 - \vartheta_{k,mel} - \vartheta_{k,blood} - \vartheta_{k,water} - \vartheta_{k,lip})$$

where $k = 1,\ldots,5$ is the layer number, $\vartheta_{k,mel}$, $\vartheta_{k,blood}$, $\vartheta_{k,water}$, and $\vartheta_{k,lip}$ are the volume fractions of melanin, blood, water, and lipids in the kth layer, and $a_{k,eu}(\lambda)$, $a_{k,ph}(\lambda)$, $a_{k,ohb}(\lambda)$, $a_{k,dhb}(\lambda)$, $a_{k,bil}(\lambda)$, $a_{k,water}(\lambda)$, $a_{k,lip}(\lambda)$ and $a_{k,\beta}(\lambda)$ are the absorption coefficients of eumelanin, pheomelanin, oxyhemoglobin, deoxyhemoglobin, bilirubin, water, lipids, and β-carotene respectively. $a_{base,\beta}(\lambda)$ is the wavelength dependent background tissue absorption coefficient and is given by $7.84e8 \times \lambda^{-3.255}$ cm^{-1}.
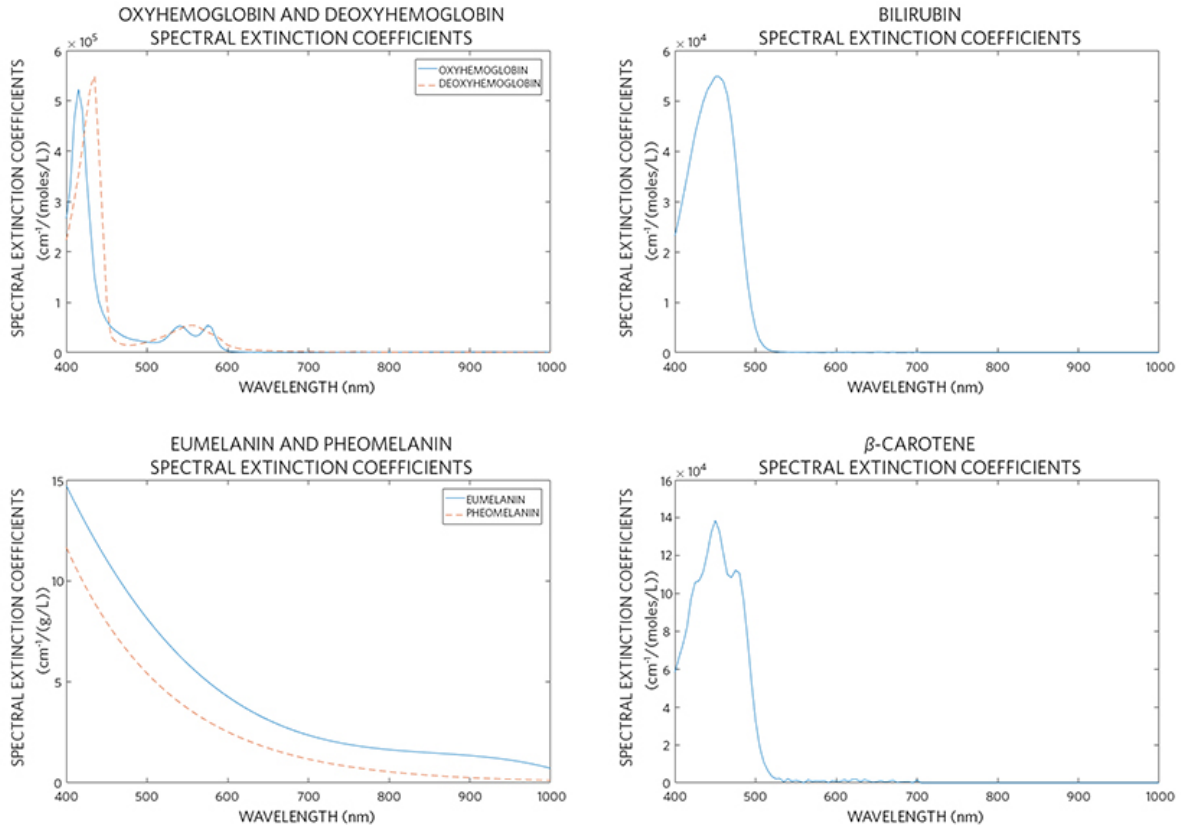

Figure 2. Spectral extinction coefficient curves for the natural pigments present in skin tissues.

The eumelanin and pheomelanin absorption coefficients are given by:

$$a_{k.eu}(\lambda) = \in_{eu}(\lambda)c_{k,eu}, \text{ and } a_{k,ph}(\lambda) = \in_{ph}(\lambda)c_{k,ph}$$

where:

$c_{k,eu}$ = eumelanin concentration (g/L) in the kth layer

$c_{k,ph}$ = pheomelanin concentration (g/L) in the kth layer

The oxyhemoglobin and deoxy hemoglobin absorption coefficients are given by:

$$a_{k.ohb}(\lambda) = \frac{\in_{ohb}(\lambda)}{66500}c_{k,hb} * \gamma , \text{ and } a_{k,dhb}(\lambda) \frac{\in_{dhb}(\lambda)}{66500} c_{k,hb} * (1 - \gamma)$$

where:

66500 = molecular weight of hemoglobin (g/mol)

$c_{k,hb}$ = hemoglobin concentration of the blood (g/L) in the kth layer

γ = ratio of oxyhemoglobin to the total hemoglobin concentration.

The absorption coefficient of bilirubin is given by:

$$a_{k,bil}(\lambda) = \frac{\epsilon_{bil}(\lambda)}{585}c_{k,bil}$$

where:

585 = molecular weight of bilirubin (g/mol)

$c_{k,bil}$ = bilirubin concentration (g/L) in the kth layer

The β-carotene absorption coefficient $a_{k,\beta}(\lambda)$ is given by:

$$a_{k,\beta}(\lambda) = \frac{\epsilon_{bil}(\lambda)}{587}c_{k,\beta}$$

where:

537 = molecular weight of β-carotene (g/mol)

$c_{k,\beta}$ = β-carotene concentration (g/L) in the kth layer

The absorption coefficient of water is given by:

$$a_{k,water}(\lambda) = \epsilon_{water}(\lambda)c_{k,water3}$$

where:

$c_{k,water}$ = water concentration (g/L) in the kth layer.

The lipid absorption coefficient is given by:

$$a_{k,lip}(\lambda) = \epsilon_{water}(\lambda)c_{k,lip3}$$

where
$c_{k,lip}$ = lipid concentration (g/L) in the kth layer.

$$a_{k,lip}(\lambda) = \epsilon_{water}(\lambda)c_{k,lip3}$$

Scattering

The total scattering coefficient for the kth layer can be defined as:

$$\mu s(\lambda) = \vartheta_{k,blood}C_k\mu s_{blood}(\lambda)+(1-\vartheta_{k,blood})\mu sT_k(\lambda).$$

where C_k is a correction factor dependent on the mean vessel diameter and the blood scattering coefficient as a function of wavelength and μsT_k is the total scattering coefficient of the bloodless tissue layer.

The following relations can be used for C_k[8]:

$$C_k = \frac{1}{1+a(0.5\,\mu s_{blood}\,d_{k,vessels})^b}$$

where $d_{k,vessels}$ is the blood vessels diameter (cm) in the kth layer. In the case of collimated illumination of the vessels the coefficients a and b have values $a = 1.007$ and $b = 1.228$. In the case of diffuse illumination of the vessels the coefficients a and b have values $a = 1.482$ and $b = 1.151$.

The total scattering coefficient of the bloodless tissue is given by[9]:

$$\mu sT_k(\lambda) = \mu s0_k\left(\frac{577nm}{\lambda}\right),$$

where $\mu s0_k$ are the scattering coefficients at the reference wavelength 577nm listed in Table 1. **Note:** μsT_k, falls monotonically with the increase in the wavelength.

The expression for the anisotropy of scattering may be constructed to include the contribution from blood[9]:

$$g_k(\lambda) = \frac{\vartheta_{k,blood}\,C_k\mu s_{blood}(\lambda)\,g_{blood}+(1-\vartheta_{k,blood})\mu sT_k(\lambda)gT(\lambda)}{\mu s_k(\lambda)},$$

where $g_k(\lambda)$ is the anisotropy factor of the bloodless tissue and

$$gT_k(\lambda) = 0.7645 + 0.2355\left[1 - \exp\left(-\frac{\lambda - 500nm}{729.1nm}\right)\right].$$

Finally, the reduced scattering coefficients is defined as $\mu s'_k(\lambda) = \mu s_k(\lambda)(1 - g_k(\lambda))$.

H2Optical Model and Computer Simulations

To determine penetration depth as a function of wavelength, Zemax OpticStudio® software was utilized. The software uses a Monte Carlo (MC) method to trace optical rays propagating in complex inhomogeneous, randomly scattering and absorbing media. Basic MC modeling of an individual photon packets trajectory consists of the sequence of the elementary simulations: photon path length generation, scattering and absorption events, reflection and/or refraction on the medium boundaries. The specular reflection from the air-tissue surface is also considered in the simulations. At the scattering site, a new photon packet direction is determined according to the Henyey-Greenstein scattering phase function:

$$f_{HG}(\Theta) = \frac{1}{4\pi}\frac{1 - g^2}{(1 + g^2 - 2g\cos\Theta)^{3/2}}$$

where Θ is the polar scattering angle. The distribution over the azimuthal scattering angle was assumed as uniform. MC technique requires values of absorption and scattering coefficients and anisotropy factor of each skin layer, its thickness and refractive index. Additionally, the mean path defined as the inverse of the scattering coefficient is required.

Results and Discussion

Using optical properties presented above, Henyey-Greenstein scattering phase function, and Zemax OpticStudio, we can simulate any biosensor configuration and determine the maximum penetration depth as a function of wavelength. For example, we have taken the following typical LED-PD biosensor configuration (**Table 2** and **Figure 3**) and skin properties shown in **Table 3**, and simulated the maximum penetration depth as a function of wavelength.

Table 2. Biosensor Configuration Used in Simulation

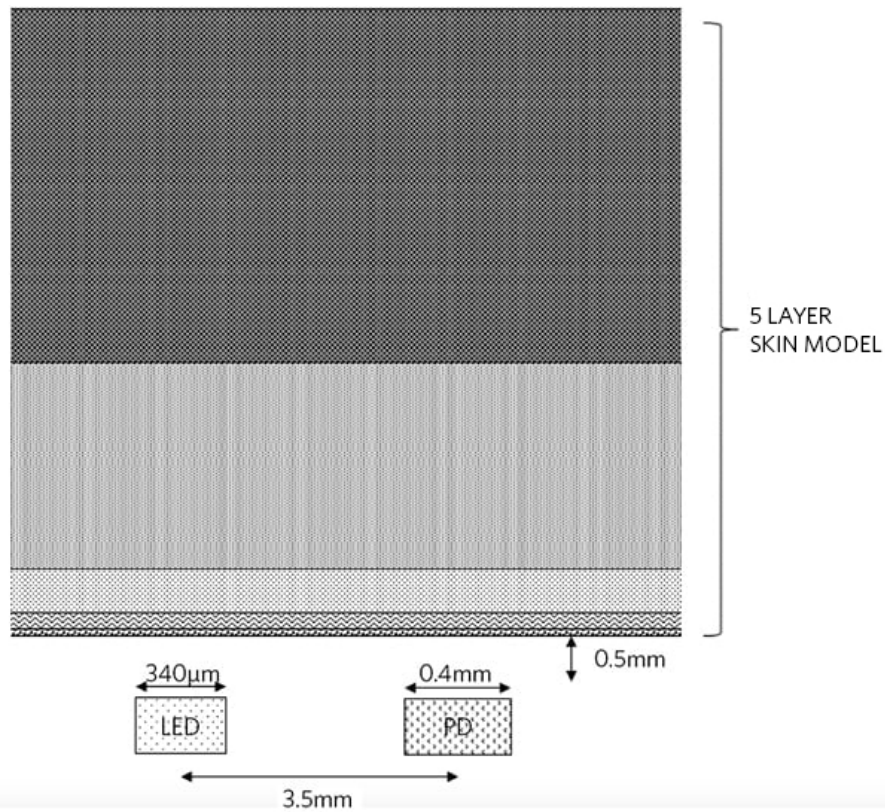| Configuration property	Value	Unit
Distance between LED and PD	3.5	mm
PD size	0.4 x 0.4	mm x mm
LED radiation pattern	Lambertian	-
LED divergence angle FWHM	60	degrees
LED size	340 x 340	µm x mm
LED/PD top to Stratum Corneum spacing	0.5	mm

Figure 3. Dimensions of biosensor configuration used in simulation.

Table 3. Skin Properties Used in Simulation

Skin layers	Volume fraction of (%)				Concentration of (g/L)				
	Melanosomes	Blood	Water	Lipids	Beta carotene	Eumelanin	Pheomelanin	Bilirubin	Hemoglobin in blood
Stratum Corneum	0.00	0.00	35.00	20.00	2.10E–04	0	0	0	0
Epidermis	1-10	0.00	60.00	15.10	2.10E–04	80	12	0	0
Papillary Dermis	0.00	0.2–4	50.00	17.33	7.00E–05	0	0	0.05	150
Reticular Dermis	0.00	0.2–5	70.00	17.33	7.00E–05	0	0	0.05	150
Subcutaneous Adipose Tissue	0.00	5.00	5.00	75–95	0	0	0	0.05	150

The absorption coefficients of the skin layers have been calculated in accordance with the presented optical model and are shown in **Figure 4**.
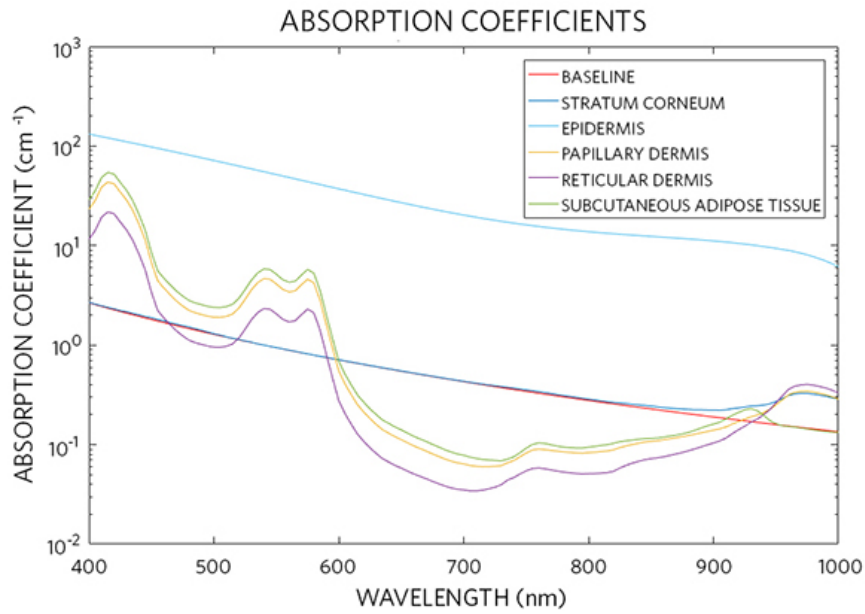
Figure 4. Absorption spectra of different skin layers calculated in accordance with the presented optical model.

The scattering coefficient, anisotropy factor, and mean path of the skin layers have been calculated in accordance with the presented model, and the result presented in **Figure 5**, **Figure 6**, and **Figure 7**.
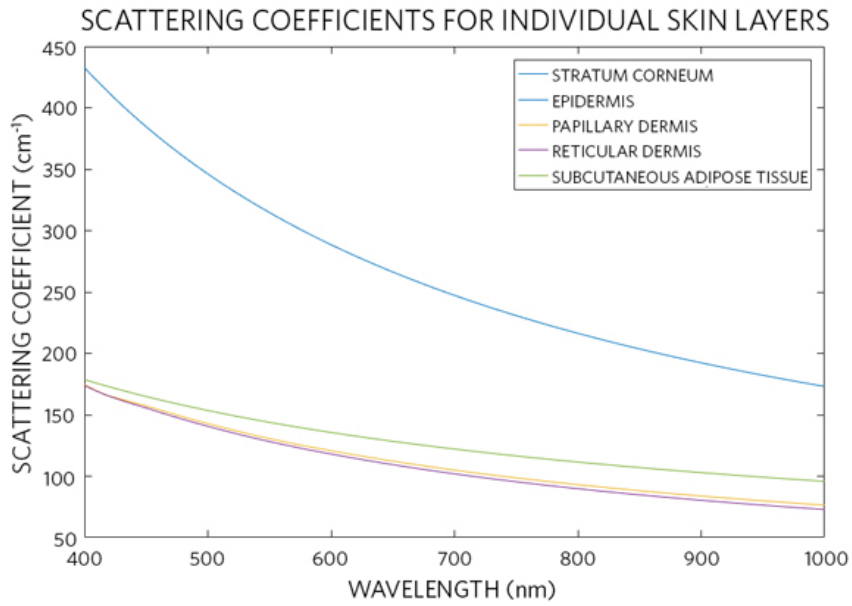

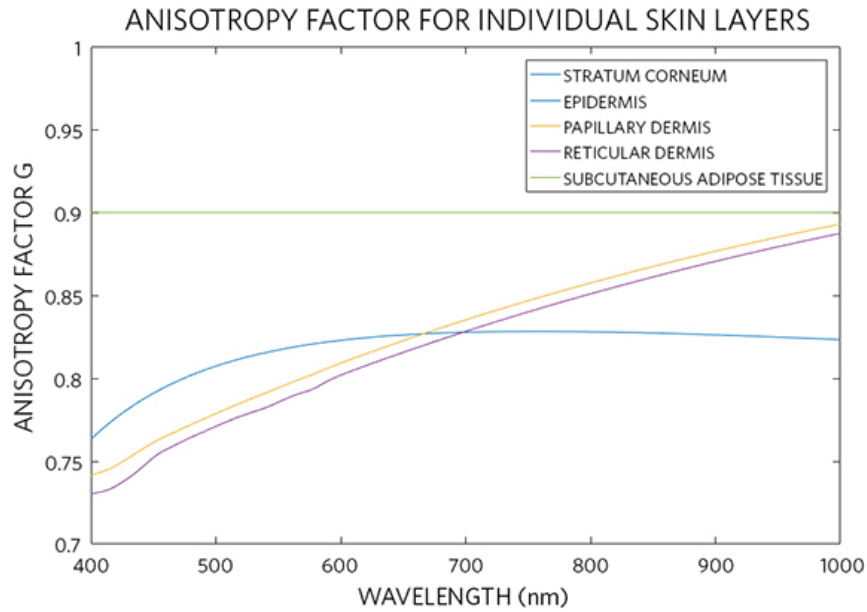*Figure 5. Scattering coefficient of different skin layers calculated in accordance with the presented optical model.*

Figure 6. Anisotropy factor of different skin layers calculated in accordance with the presented optical model.
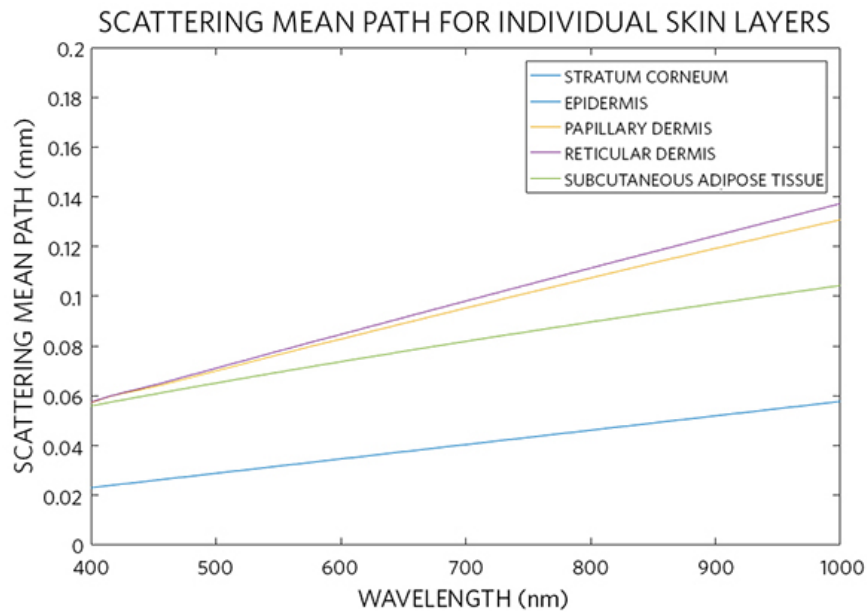
. Figure 7. Scattering mean path of different skin layers calculated in accordance with the presented optical model

The penetration depth of light into a biological tissue is an important parameter used to determine the performance of a biosensor. Penetration depth is the distance into the skin that the light has traveled. Simulation of the optical penetration depth has been performed with the absorption .and reduced scattering coefficient values presented above. Simulation results are shown in **Figure 8**
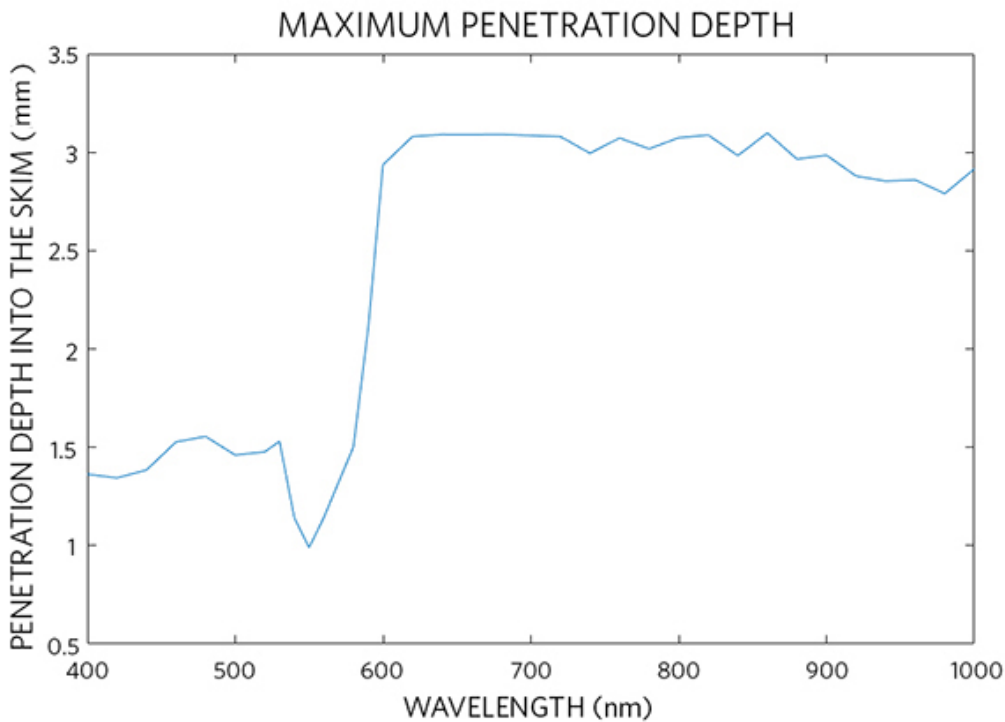
Figure 8. Simulated maximum penetration depth for the situation given in Figure 3 and Table 3.

Conclusion

In this article, we have modeled human skin tissue with a five-layer structure where each layer represents its corresponding anatomical layer. To simulate light tissue interaction, the biological characteristics of each layer is moded with three wavelength-dependent numbers, absorption coefficient, scattering coefficient, and anisotropy factor. Then, we have used a commercial ray tracing software to calculate penetration depth of light into skin tissue for simulating the performance of optical biosensor architectures.

References

1. K. S. Stenn, "The skin, " Cell and Tissue Biology ed. by L. Weiss, Baltimore: Urban & Shwarzenberg, 541-572 (1988).
2. M. R. Chedekel, "Photophysics and Photochemistry of Melanin, " In: L. Zeise, M. R. Chedekel and T. B. Fitzpatrick, Eds., Melanin: Its Role in Human Photoprotection, Valdenmar, Overland Park, pp. 11-22 (1994).
3. T. J. Ryan, "Cutaneous Circulation," in Physiology, Biochemistry, and Molecular Biology of the Skin, 1, ed. by L.A. Goldsmith, Oxford University Press, Oxford (1991).
4. A. Zourabian, A. Siegel, B, Chance, N. Ramanujan, M. Rode and D. A. Boas, "Trans-abdominal monitoring of fetal arterial blood oxygenation using pulse oximetry, " J. Biomed. Opt. **5** 391–405 (2000).
5. T. Hamaoka *et al,* "Quantification of ischemic muscle deoxygenation by near infrared time-resolved spectroscopy, " J. Biomed. Opt. 5 102–5 (2000).
6. M. I. Gurr, R. T. Jung, M. P. Robinson and W. P. T. James, "Adipose tissue cellularity in man: the relationship between fat cell size and number, the mass and distribution of body fat and the history of weight gain and loss," Int. J. Obesity **6** 419–36 (1982).
7. Y. Taton "Obesity, Pathphysiology, Diagnostics, Therapy"*,* Warsaw: Medical Press (1981).
8. W. Verkruysse, G. W. Lucassen, J. F. de Boer, D. J. Smithies, J. S. Nelson, M. J. C. van Gemert, "Modelling light distributions of homogeneous versus discrete absorbers in light irradiated turbid media," Phys. Med. Biol. **42**, 51-65 (1997).
9. G. Altshuler, M. Smirnov, I. Yaroslavsky, "Lattice of optical islets: a novel treatment modality in photomedicine," Journal of Physics D: Applied Physics **38**, 2732-2747 (2005).

OpticStudio is a registered trademark of Zemax, LLC.

Related Parts		
MAX30101	High-Sensitivity Pulse Oximeter and Heart-Rate Sensor for Wearable Health	Free Samples
MAX30102	High-Sensitivity Pulse Oximeter and Heart-Rate Sensor for Wearable Health	Free Samples
MAX86160	Integrated Heart-Rate Sensor for In-Ear Applications	Free Samples